STATUS OF THE TESLA POWER COUPLER DEVELOPMENT PROGRAMME IN FRANCE

S. Chel, M.Desmons, C. Travier, DSM/DAPNIA/SEA, CEA Saclay, 91191 Gif-sur-Yvette
T. Garvey, P. Lepercq, R. Panvier, CNRS/IN2P3/LAL, 91405 Orsay
S. Bulher, G. Guillier, CNRS/IN2P3/IPN, 91405 Orsay

Abstract

As part of the R&D effort of the TTF collaboration, an input power coupler development programme has been undertaken by a CEA/DSM and CNRS/IN2P3 collaboration [1]. The power test stand which includes a cryostat is described and the cryogenic performances of the cryostat are presented. The results of the test of a tapered coaxial waveguide are given. The $\lambda/2$ ceramic window is described and TiN coating characterisation is presented.

1 INTRODUCTION

For the present TESLA design, based on 25 MV/m 9-cell cavities, main couplers have to handle an RF power of 208 kW. If superstructures [2] are used, one coupler could power up to eight 7-cell cavities and thus require increased handling capabilities up to 1.3 MW. Working at 40 MV/m as required for TESLA upgrades to higher energies would mean even larger input power. These reasons, together with the need to reduce the cost, necessitate the design of a new coupler. This paper presents the work done in this framework: the construction of a power test stand including a cryostat, the first tests of coupler components and the design of a new window.

2 POWER TEST STAND

The power test stand [1] consists of a 1 MW, 800 μs L-band klystron that delivers power to a 5 m long waveguide system. This waveguide can be either short-circuited, thus allowing one to establish a standing wave pattern with the possibility of displacing the nodes of the electric field by varying the frequency, or matched to operate in the travelling wave regime. The acquisition of vacuum, RF, electron and light emission signals is done for each RF pulse via a Labview application running on a PC computer. The test stand was operated in 1997 for the test of a doorknob waveguide to coax transition, a tapered ϕ60-ϕ40 coaxial waveguide, a conical type ceramic window and an antenna type waveguide to coax transition. All these tests were performed at room temperature. At the beginning of 1998, the experiments were stopped to upgrade the test stand by adding a cryostat as described below.

2.1 Description of the cryostat

In order to test the coupler in a more realistic environment, the cryostat shown in figure 1 has been built. It allows

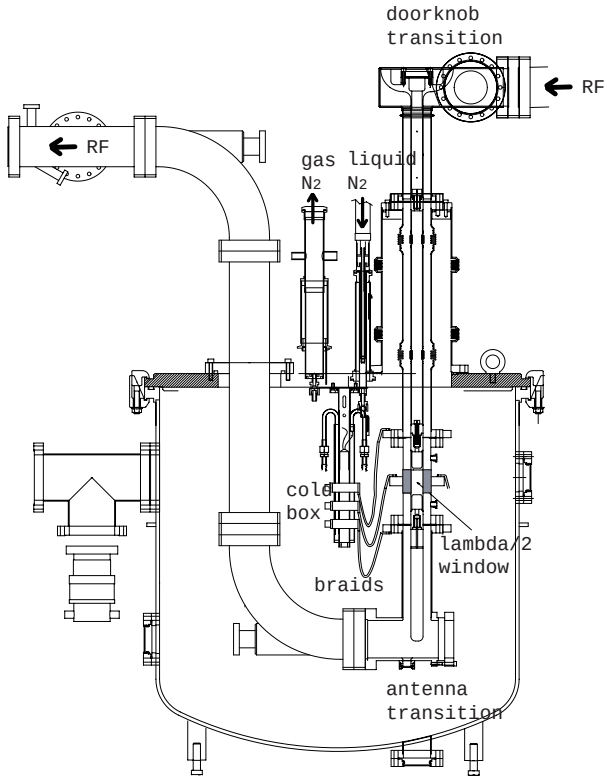

Figure 1: Mechanical drawing showing a cut of the cryostat (the copper screen is not represented)

one to maintain the cold window at 80 K, while the upper waveguide to coax transition is at room temperature, as in a real coupler. The refrigeration principle is based on a continuous evaporation of liquid nitrogen flowing through a cooling box. Three copper braids connect the two flanges of the window and a copper ring brazed or clamped around it, to the cold box. A copper screen shields the entire cold part in order to protect it from radiation coming from the tank. The pipe guiding the cold vapour to the output heater is brazed on to the copper screen to thermalize it at 80 K. The liquid nitrogen flow is regulated to maintain a constant temperature at the exit of the circuit.

The temperature measurements used to control the system operation are done with platinum probes (100 Ω). In order to estimate the RF power dissipated in the window, two methods are available:

- thermal flux measurement: when there is a thermal flux $\dot{Q}$ flowing across one of the copper braids linking

the window and the cooling box, a temperature difference ΔT is established across this braid. If L is the length of the braid, A its section and λ the thermal conductivity, then we have: $\Delta T = \dot{Q} L (\lambda A)^{-1}$. In our case, ΔT = 5.2 K/W.

- flow measurement: the power dissipated in the window leads to an additional nitrogen consumption. By measuring the gas flow at the exit of the nitrogen circuit, one can estimate the refrigeration power $\dot{Q}$ as: $\dot{Q} = \dot{M} \Delta H_i^o = \dot{M}(l_v + c_p \Delta T_{vap})$, where $\dot{M}$ is the mass flow, ΔH_i^o the enthalpy difference between the input and output, l_v the latent heat of vaporisation, c_p the specific heat of vapour and ΔT_{vap} the overheating of the saturated vapour.

The window can be baked in situ inside the cryostat up to a temperature of 150°C, with the help of three 75 W heating resistances. During this process, it is necessary to cool the cold box in order to prevent the melting of the lead braze.

During the cool down of the cryostat, one would like to avoid cryopumping the residual gas on the ceramic. This is done by maintaining the ceramic a few degrees higher than the nearest metal pieces so that the cryopumping is done preferentially on the metallic surfaces.

2.2 Test of the cryostat

The cooling down of the cryostat takes from 7 to 10 hours to reach temperatures lower than 100 K and 12 to 16 hours to reach a temperature stabilisation allowing calorimetric measurements. The nitrogen consumption for one cool-down is between 17 and 20 litres. When the steady state is reached, the static consumption of liquid nitrogen is 0.6 l/h if the copper screen is thermalized to 86 K (necessary for precise thermal measurements) and 0.43 l/h if the screen is not thermalized (temperature around 165 K).

The bakeout temperature of 150°C was easily reached at the ceramic with a heating power of 3 times 75 W, while maintaining the room temperature at the cooling box.

The two methods proposed earlier to measure the dissipated RF power were tested by simulating the RF losses with a known heating power. It was verified that there is a good proportionality between the heater power and the temperature difference at both ends of the braids, measured with platinum probes. The proportionality coefficient measured at the upper, middle and lower braid were respectively 4.7, 5.0 and 4.6 K/W, for a theoretical value of 5.2 K/W. The calorimetry done with the gas flow rate measurement leads to a value of 16.9 l/h/W for a theoretical value of 15.6 l/h/W. These methods require several hours waiting so that the thermal equilibrium is reached, before doing any meaningful measurement.

3 POWER TEST OF A TAPERED COAXIAL TRANSITION

One of the tests done on the test stand concerned a tapered coaxial waveguide used to match the ϕ60 mm coaxial waveguide of the coupler to the ϕ40 mm coupler port of the TESLA 9-cell cavity. This tapered waveguide was tested in the standing wave regime, with 500 μs RF pulses. Figure 2 shows the vacuum and photomultiplier signals as a function of input RF power. These pictures show that below 500 kW, multipactor occurs at all power levels (The vertical lines that can be distinguished on the plots are due to the fact that the power ramping is done with a 50 kW step). This was confirmed by localised heating of the tapered waveguide. Electron trajectory simulations made in reference [3] lead to the possible conclusion that such a tapered coaxial guide could be "used to reduce multipacting". This experiment apparently shows that this is not the case thus demonstrating that electron trajectory simulations are not yet sufficient to predict multipacting behaviours.

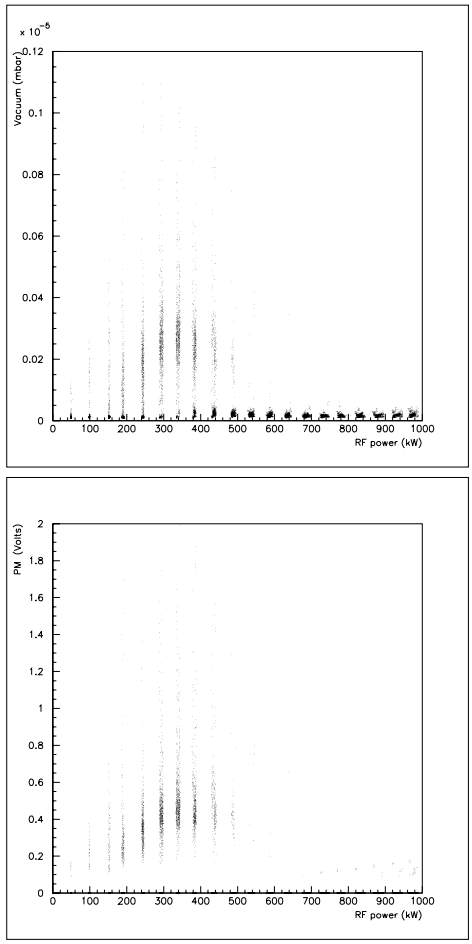

Figure 2: Tapered coaxial guide: Vacuum (top) and Photomultiplier (bottom) signals vs. RF power

4 COLD WINDOWS

In view of reducing coupler costs, it was decided to test different window designs starting from the simplest ones. The first window designed and constructed is a $\lambda/2$ window, where the ceramic thickness is chosen to be a half wavelength thus ensuring the matching. This window has the advantage of being rather simple, and to have no longitudinal electric field at the ceramic surface (and therefore to be theoretically multipactor free), but has the drawback of having a relatively low bandwidth (131 MHz for a reflection coefficient less than 0.2) and to be quite lossy due to the large ceramic thickness (3.84 cm). In order to reduce the cost, it was decided to have only one high temperature brazing. The inner conductor is made of copper, while the outer conductor is made of kovar which is a typical alloy used in ceramic/metal assemblies. The kovar piece is then TIG welded to the stainless steel copper coated outer conductor. Figure 3 shows the photograph of a the ceramic brazed to the outer and inner conductors. Since the maximum electric field is on the inner conductor, one should be careful that the braze does not leak, or if it does, the extra metal should be removed by machining the piece. Two $\lambda/2$ windows were fabricated by SICN [4] and are now ready to be tested. Travelling wave windows were also designed and will soon be fabricated.

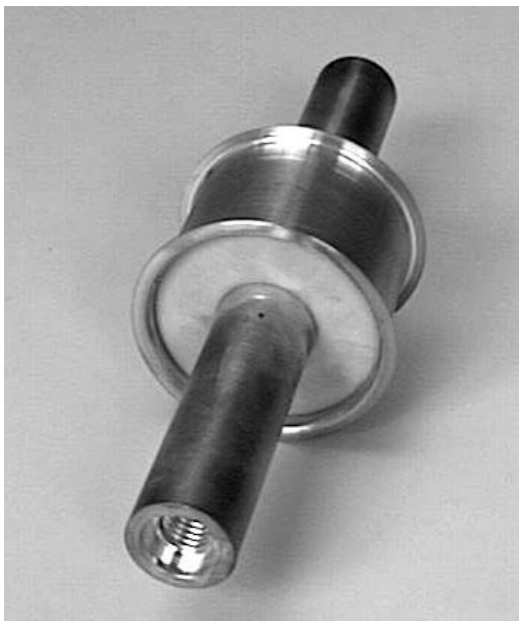

Figure 3: Photograph of the ceramic brazed to the inner and outer conductors

5 TITANIUM NITRIDE COATING

It is customary to coat the ceramic with a thin layer (typically a few nanometers) of titanium nitride, in order to reduce its secondary emission coefficient. The difficulty of the coating is to precisely control the coating thickness and stoechiometry. We made thickness measurements with a quartz balance inside the magnetron and Rutherford Backscattered Spectroscopy (RBS) to analyze the composition of the coating and also control the thickness. Figure 4 shows the thickness measured by both methods as a function of the coating time. For the desired coating thickness of 10 nm, the coating time with the present operating conditions is around 100 s. These tests showed us that resistance is not the right parameter to characterise coating thickness. The coating conditions used so far do not allow to obtain stoechiometric TiN, and lead to a high oxygen content. Studies will be continued to improve this situation.

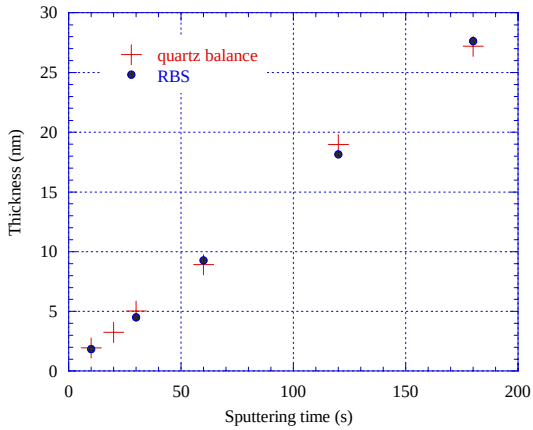

Figure 4: Coating thickness versus sputtering time

6 CONCLUSION

The complete power test stand including the cryostat is now ready to be used. The $\lambda/2$ window will soon be tested both at room and liquid nitrogen temperature. A complete coupler design is underway that should lead to a first prototype in early 1999.

7 ACKNOWLEDGEMENTS

We would like to thank all the people that participated to the work described above at CEA, LAL, IPN and SICN. We are especially grateful to Pr. Trouslard and his team S. Pellegrino and L. Beck for performing the RBS analysis at the INSTN Van de Graaff accelerator, and for lending us the quartz balance.

8 REFERENCES

[1] Chel S. et al., Proceedings of the Fifth EPAC, June 10-14, 1996, Sitges, pp. 2088-2090.

[2] Sekutowicz J., Ferrario M., C. Tang, Superconducting Superstructures for the TESLA Collider, TESLA 98-08, DESY, April 1998.

[3] Somersalo E. et al., Particle Accelerators, vol. 59, pp. 107-141, 1998.

[4] SICN, BP 1, 38113, Veurey-Voroize, France.